

Lanthanide versus Actinide Reactivity in the Formation of Sterically Crowded $[(C_5Me_5)_3ML_n]$ Nitrile and Isocyanide Complexes

William J. Evans,* Thomas J. Mueller, and Joseph W. Ziller^[a]

Abstract: The limits of steric crowding in organometallic metallocene complexes have been examined by studying the synthesis of $[(C_5Me_5)_3ML_n]$ complexes as a function of metal in which $L = Me_3CCN$, Me_3CNC , and Me_3SiCN . The bis(*tert*-butyl nitrile) complexes $[(C_5Me_5)_3Ln(NCCMe_3)_2]$ ($Ln = La$, **1**; Ce , **2**; Pr , **3**) can be isolated with the largest lanthanide metal ions, La^{3+} , Ce^{3+} , and Pr^{3+} . The Pr^{3+} ion also forms an isolable mono-nitrile complex, $[(C_5Me_5)_3Pr(NCCMe_3)]$ (**4**), whereas for Nd^{3+} only the mono-adduct $[(C_5Me_5)_3Nd(NCCMe_3)]$ (**5**) was observed. With smaller metal ions,

Sm^{3+} and Y^{3+} , insertion of Me_3CCN into the $M-C(C_5Me_5)$ bond was observed to form the cyclopentadiene-substituted ketimide complexes $[(C_5Me_5)_2Ln\{NC(C_5Me_5)(CMe_3)\}(NCCMe_3)]$ ($Ln = Sm$, **6**; Y , **7**). With *tert*-butyl isocyanide ligands, a bis-isocyanide product can be isolated with lanthanum, $[(C_5Me_5)_3La(CNCMe_3)_2]$ (**8**), and a mono-isocyanide product with neodymium, $[(C_5Me_5)_3Nd-$

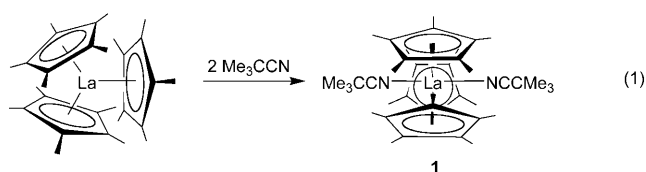
$(CNCMe_3)]$ (**9**). Silicon-carbon bond cleavage was observed in reactions between $[(C_5Me_5)_3Ln]$ complexes and trimethylsilyl cyanide, Me_3SiCN , to produce the trimeric cyanide complexes $\{[(C_5Me_5)_2Ln(\mu-CN)(NCSiMe_3)]_3\}$ ($Ln = La$, **10**; Pr , **11**). With uranium, a mono-nitrile reaction product, $[(C_5Me_5)_3U(NCCMe_3)]$ (**12**), which is analogous to **5**, was obtained from the reaction between $[(C_5Me_5)_3U]$ and Me_3CCN , but $[(C_5Me_5)_3U]$ reacts with Me_3CNC through C–N bond cleavage to form a trimeric cyanide complex, $\{[(C_5Me_5)_2U(\mu-CN)(CNCMe_3)]_3\}$ (**13**).

Keywords: actinides • cyanides • cyclopentadienyl ligands • lanthanides • metallocenes

Introduction

For many years, it was believed that $[(C_5Me_5)_3M]$ complexes were too sterically crowded to exist.^[1,2] However, the isolation of $[(\eta^5-C_5Me_5)_3M]$ complexes with $M = La$,^[3] Ce ,^[4] Pr ,^[4] Nd ,^[5] Sm ,^[6] Gd ,^[7] Y ,^[7] and U ,^[8] dispelled this idea. Subsequently, studies with $[(C_5Me_5)_3U]$ demonstrated that it was possible with uranium to synthesize tris(pentamethylcyclopentadienyl) complexes that contained a fourth ligand in the coordination sphere: $[(C_5Me_5)_3UF]$,^[9] $[(C_5Me_5)_3UCl]$,^[9] $[(C_5Me_5)_3UMe]$,^[10] $[(C_5Me_5)_3U(CO)]$,^[11] and $[(C_5Me_5)_3U(N_2)]$.^[12] Recent studies of the reactivity of $[(C_5Me_5)_3La]$ in the presence of Lewis bases revealed that tris(pentamethylcyclopentadienyl) complexes could also be

isolated with two additional ligands attached to the metal [Eq. (1)].^[13] This showed that steric limits were still being defined in the $[(C_5Me_5)_3M]$ system.



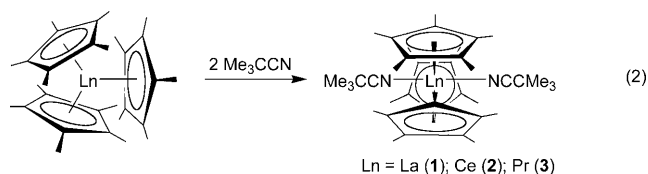
In this paper, we explore the generality of the synthesis in Equation (1) by making comparisons between lanthanides and uranium as well as within the lanthanide series as a function of metal size. Since lanthanum is the largest trivalent metal in the periodic table, it was sterically best suited to generate a $[(C_5Me_5)_3ML_2]$ complex. It was uncertain if analogues of $[(C_5Me_5)_3La(NCCMe_3)_2]$ could be made with smaller metals and uranium or if other types of reactivity would be observed due to the steric crowding. Reactions with isocyanides as well as nitriles are reported.

[a] Prof. W. J. Evans, T. J. Mueller, Dr. J. W. Ziller
Department of Chemistry, University of California
Irvine, California 92697-2025 (USA)
Fax: (+1) 949-824-2210
E-mail: wevans@uci.edu

Supporting information for this article, which includes X-ray data collection, structure solution, and refinement of compounds **2–5**, **8**, **9**, and **11–13**, is available on the WWW under <http://dx.doi.org/10.1002/chem.200901990>.

Results

$[(C_5Me_5)_3Ln(NCCMe_3)_2]$ ($Ln = Ce$, **2; Pr , **3**):** Examination of reactions analogous to the synthesis of $[(C_5Me_5)_3La(NCCMe_3)_2]$ (**1**) in Equation (1) with cerium and praseodymium showed that these slightly smaller metals would also form $[(C_5Me_5)_3Ln(NCCMe_3)_2]$ complexes ($Ln = Ce$, **2**; Pr , **3**) in quantitative yield [Eq. (2)].



Complexes **2** and **3**, like complexes **4–10**, described later in this paper, were characterized by 1H NMR, ^{13}C NMR, and IR spectroscopy as well as by elemental analysis. X-ray crystallography was also used to identify **2** and **3** (Figure 1). Complexes **2** and **3** are isomorphous with **1** and also have IR spectra that are nearly identical to that of **1** ($\tilde{\nu} = 2256\text{ cm}^{-1}$);^[13] the C–N stretches in **2** and **3** are both observed at 2255 cm^{-1} compared with 2231 cm^{-1} in the free nitrile.^[14] X-ray data collection parameters for complexes **2** and **3** are listed in Table 1 and metrical parameters are described in the structural section below.

$[(C_5Me_5)_3Ln(NCCMe_3)]$ ($Ln = Pr$, **4; Nd , **5**):** Attempts to make a $[(C_5Me_5)_3LnL_2]$ complex with the next smallest lanthanide, neodymium, by adding excess Me_3CCN to $[(C_5Me_5)_3Nd]$ formed the mono-nitrile adduct $[(C_5Me_5)_3Nd(NCCMe_3)]$ (**5**) in quantitative yield [Eq. (3)].

Complex **5** is the first tris(pentamethylcyclopentadienyl) lanthanide complex isolated with one additional ligand; this $[(C_5Me_5)_3ML]$ class had previously been known only with

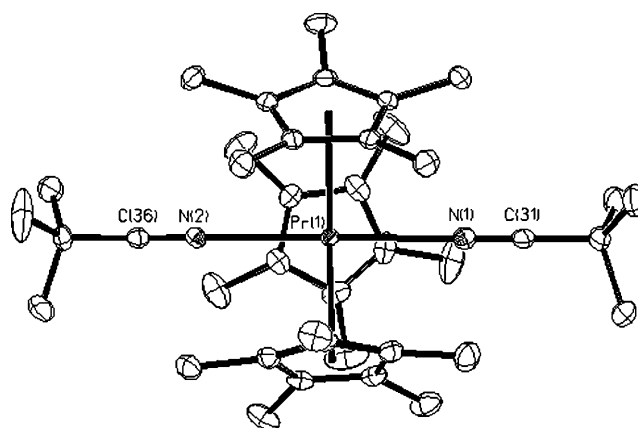
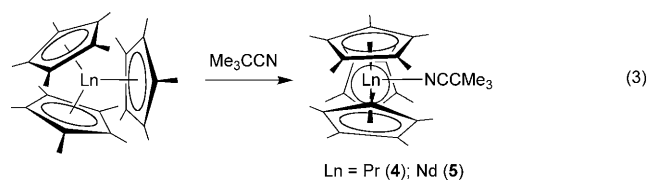


Figure 1. Thermal ellipsoid plot of complex **3** drawn at the 50% probability level. Hydrogen atoms and benzene solvent molecules have been omitted for clarity. See Figure S1 in the Supporting Information for a thermal ellipsoid plot of complex **2**.



uranium.^[11,12] Isolation of the mono-nitrile adduct with Nd suggested that metals smaller than Pr would not form bis-nitrile adducts with Me_3CCN .

To explore this mono-/bis-nitrile borderline further, a stoichiometric reaction of Me_3CCN with $[(C_5Me_5)_3Pr]$ was conducted and the mono-nitrile praseodymium adduct $[(C_5Me_5)_3Pr(NCCMe_3)]$ (**4**) was isolated, again in quantitative yield [Eq. (3)]. Attempts to make La and Ce analogues of **4** and **5** using stoichiometric amounts of the nitrile gave only the bis-nitrile complexes **1** and **2**. Hence, synthetically,

Table 1. X-ray data collection parameters for complexes **2–5**.

	2	3	4	5
formula	$C_{40}H_{63}N_2Ce \cdot C_6H_6$	$C_{40}H_{63}N_2Pr \cdot C_6H_6$	$C_{35}H_{54}NPr \cdot 2(C_6H_6)$	$C_{35}H_{54}NNd \cdot 2(C_6H_6)$
M_r	790.15	790.94	785.92	789.25
space group	$P2_1/c$	$P2_1/c$	$P2_1/c$	$P2_1/c$
crystal system	monoclinic	monoclinic	monoclinic	monoclinic
a [Å]	19.122(2)	19.110(2)	18.563(4)	18.513(1)
b [Å]	17.527(2)	17.478(2)	17.695(4)	17.680(1)
c [Å]	13.066(1)	12.990(1)	12.769(3)	12.7578(7)
V [Å ³]	4284.5(8)	4246.9(6)	4179.2(17)	4161.0(4)
α [°]	90	90	90	90
β [°]	101.920(1)	101.795(1)	94.890(3)	94.829(1)
γ [°]	90	90	90	90
Z	4	4	4	4
ρ_{calcd} [Mg m ⁻³]	1.225	1.237	1.249	1.260
μ [mm ⁻¹]	1.093	1.178	1.197	1.279
T [K]	153(2)	103(2)	153(2)	143(2)
R_1 [$I > 2\sigma(I)$] ^[a]	0.0372	0.0276	0.0505	0.0240
wR_2 (all data) ^[a]	0.1093	0.0668	0.1478	0.0618

[a] Definitions: $wR_2 = [\Sigma[w(F_o^2 - F_c^2)^2] / \Sigma[w(F_o^2)^2]]^{1/2}$, $R_1 = \Sigma||F_o| - |F_c|| / \Sigma|F_o|$.

praseodymium is the element at which the bis to mono switchover occurs and both types of complexes are accessible.

Complexes **4** and **5** were characterized by spectroscopic and analytical methods and by X-ray crystallography (Figure 2). Complexes **4** and **5** are isomorphous and have

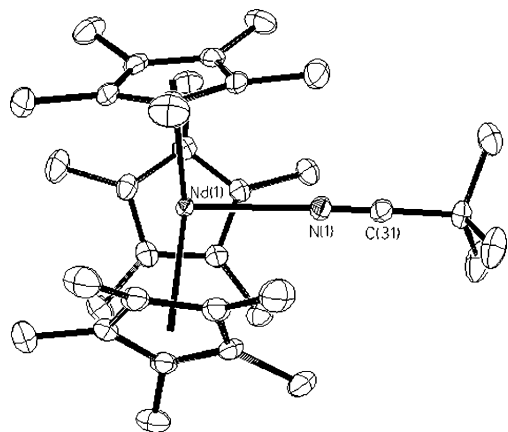
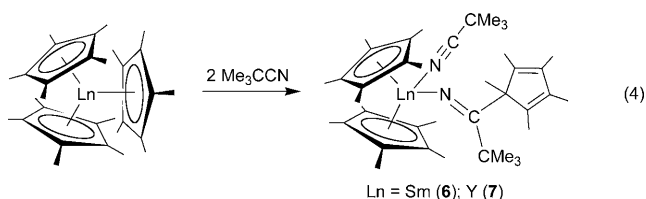


Figure 2. Thermal ellipsoid plot of complex **5** drawn at the 50% probability level. Hydrogen atoms and benzene solvent molecules have been omitted for clarity. See Figure S2 in the Supporting Information for a thermal ellipsoid plot of complex **4**.

nearly identical IR spectra: the nitrile C–N stretches in **4** and **5** are observed at 2255 and 2256 cm^{−1}, respectively. Metrical parameters are described in a later section.

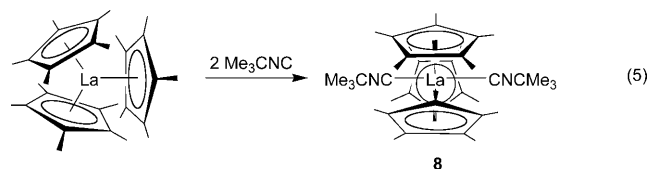
[(C₅Me₅)₂Ln{NC(C₅Me₅)(CMe₃)}(NCCMe₃)] (Ln = Sm, **6; Y, **7**):** The *tert*-butyl nitrile chemistry of the next smallest lanthanide, promethium, was not examined because it is radioactive. A preliminary study of the [(C₅Me₅)₃Ln]/Me₃CCN reaction with the next member of the series, samarium,^[15] suggested that nitrile insertion into the Sm–C(C₅Me₅) linkage occurred to yield [(C₅Me₅)₂Sm{NC(C₅Me₅)(CMe₃)}(NCCMe₃)] (**6**) [Eq. (4)].



The reaction has been fully examined by ¹H NMR, ¹³C NMR, and IR spectroscopy as well as elemental analysis and is consistent with the product shown in Equation (4). PhCN forms a complex analogous to **6** that has been fully characterized by X-ray crystallography.^[16] The orange color of **6** appeared immediately on mixing the reagents, even at low temperature.

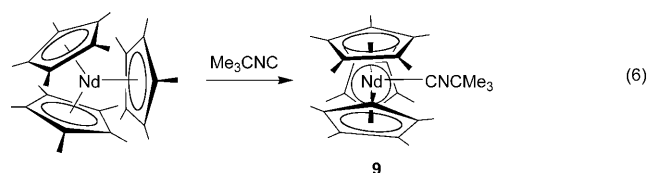
As shown in Equation (4), the smaller metal, yttrium, reacts similarly to samarium to form [(C₅Me₅)₂Y{NC(C₅Me₅)(CMe₃)}(NCCMe₃)] (**7**), which was characterized by analytical and spectroscopic methods. The ¹H NMR spectrum of diamagnetic **7** displayed three resonances (δ = 2.14, 1.89, 1.30 ppm) in a 1:2:2 ratio consistent with the insertion of the nitrile substrate into an Y–C(C₅Me₅) bond.^[13] Complexes **6** and **7** have similar IR spectra; each contains two different C–N stretches. The absorptions observed at 2262 and 2264 cm^{−1}, similar to that of the free nitrile, are assumed to be the coordinated nitrile stretches in **6** and **7**, respectively, whereas the absorptions at 1624 and 1628 cm^{−1}, in the range observed for C=N double bonds, appear to be the C–N stretches of the inserted nitrile for each complex.

[(C₅Me₅)₃La(CNCMe₃)₂] (8**):** Once the synthesis of complexes **1–5** was well established, reactions with the sterically similar isocyanide, Me₃CNC, were examined to determine the effect of changing the donor atom from nitrogen to carbon. [(C₅Me₅)₃La] reacts, as in Equation (1), with excess Me₃CNC to produce a bis-isocyanide adduct, **8**, in quantitative yield [Eq. (5)].



The structure of complex **8**, determined by X-ray crystallography, is shown in Figure 3. X-ray data collection parameters for complex **8** are shown in Table 2.

As in the Me₃CCN reaction [Eq. (3)], [(C₅Me₅)₃Nd] reacts with excess Me₃CNC to produce the mono(ligand) adduct, [(C₅Me₅)₃Nd(CNCMe₃)] (**9**) in quantitative yield [Eq. (6)].



The structure of **9** determined by X-ray crystallography is shown in Figure 4. The C–N stretches in **8** and **9** are observed at 2168 and 2178 cm^{−1}, respectively, compared with 2131 cm^{−1} in the free isocyanide.^[17] This is consistent with the isocyanide acting as a σ donor. The isolation of **8** and **9** shows that the formation of [(C₅Me₅)₃LnL_n] complexes is not limited to L = Me₃CCN.

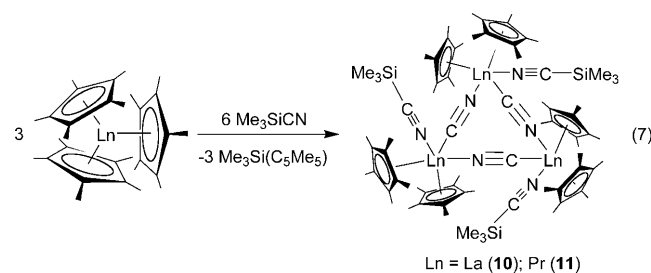
[(C₅Me₅)₂Ln(μ-CN)(NCSiMe₃)₃] (Ln = La, **10; Pr, **11**):** When a reaction analogous to Equation (1) was examined

Table 2. X-ray data collection parameters for complexes **8**, **9**, **11**, **12**, and **13**.

	8	9	11	12	13
formula	C ₄₀ H ₆₃ N ₂ La·C ₆ H ₆	C ₃₅ H ₅₄ NNd·2 (C ₆ H ₆)	C ₇₅ H ₁₁₇ N ₆ Pr ₃ Si ₃ ·2 (C ₆ H ₆)	C ₃₅ H ₅₄ NU·2 (C ₆ H ₆)	C ₇₈ H ₁₁₇ N ₆ U ₃ ·3.5 (C ₆ H ₆)
<i>M_r</i>	788.94	789.25	1765.96	883.04	2126.24
space group	<i>P</i> 2 ₁ / <i>c</i>	<i>P</i> 2 ₁ / <i>c</i>	<i>P</i> 6 ₃ / <i>m</i>	<i>P</i> 2 ₁ / <i>c</i>	<i>P</i> 1̄
crystal system	monoclinic	monoclinic	hexagonal	monoclinic	triclinic
<i>a</i> [Å]	19.213(1)	18.5295(13)	18.083(2)	18.531(9)	13.731(1)
<i>b</i> [Å]	17.667(1)	17.6674(12)	18.083(2)	17.600(8)	15.506(1)
<i>c</i> [Å]	12.9940(9)	12.7086(9)	15.659(3)	12.791(6)	24.681(2)
<i>V</i> [Å ³]	4315.6(5)	4146.5(5)	4434(1)	4156(3)	4704.4(6)
<i>α</i> [°]	90	90	90	90	86.775(1)
<i>β</i> [°]	101.918(1)	94.6864(9)	90	94.943(6)	74.209(1)
<i>γ</i> [°]	90	90	120	90	68.660(1)
<i>Z</i>	4	4	2	4	2
<i>ρ</i> _{calcd} [Mg m ⁻³]	1.214	1.264	1.323	1.411	1.501
<i>μ</i> [mm ⁻¹]	1.021	1.283	1.706	3.936	5.197
<i>T</i> [K]	153(2)	103(2)	103(2)	153(2)	153(2)
<i>R</i> ₁ [<i>I</i> > 2σ(<i>I</i>)] ^[a]	0.0228	0.0194	0.0503	0.0485	0.0280
<i>wR</i> ₂ (all data) ^[a]	0.0618	0.0488	0.1239	0.1055	0.0697

[a] Definitions: $wR_2 = [\sum[w(F_o^2 - F_c^2)^2]/\sum[w(F_o^2)^2]]^{1/2}$, $R_1 = \sum||F_o| - |F_c||/\sum|F_o|$.

with Me₃SiCN, reduction was observed [Eq. (7)] rather than adduct formation to form complexes like **1–5**.



The cyanide complex $[(C_5Me_5)_2La(\mu-CN)(NCSiMe_3)]_3$ (**10**) was isolated and identified by ¹H NMR spectroscopy and X-ray crystallography. In addition, Me₃SiC₅Me₅^[18] was isolated and identified by ¹H NMR spectroscopy. Complex **10** had previously been made from the reaction of an isocyanamide and Me₃SiCN [Eq. (8)].^[19]

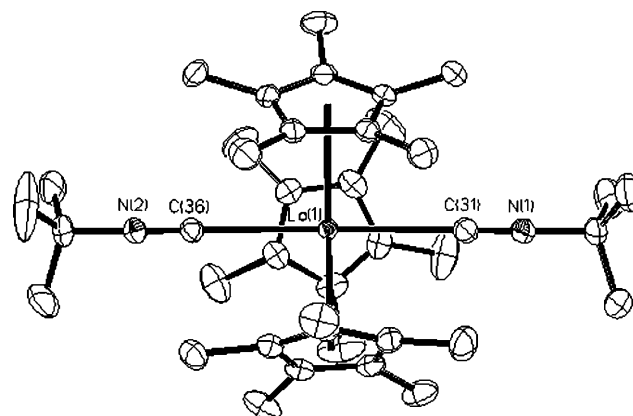
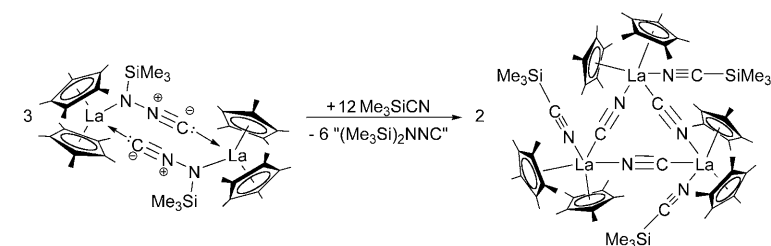


Figure 3. Thermal ellipsoid plot of complex **8** drawn at the 50% probability level. Hydrogen atoms and benzene solvent molecules have been omitted for clarity.

The reaction in Equation (7) can be rationalized by the sterically induced reduction (SIR) reactivity that had been firmly established for $[(C_5Me_5)_3M]$ complexes in which the $(C_5Me_5)^-$ ring acts as a reductant according to Equation (9).^[1,2,4,7,20]



With praseodymium, reactivity analogous to that of lanthanum in Equation (7) was observed to produce $[(C_5Me_5)_2Pr(\mu-CN)(NCSiMe_3)]_3$ (**11**). Complex **11** is isomorphous with **10** (Figure 5). Me₃SiC₅Me₅ was again isolated as a byproduct and identified by ¹H NMR spectroscopy.

However, these SIR reactions normally give $(C_5Me_5)_2$ as the isolated byproduct. The isolation of Me₃SiC₅Me₅ as a byproduct in Equation (7) requires that the C₅Me₅ radical product of Equation (9) be trapped by the cleaved Me₃Si

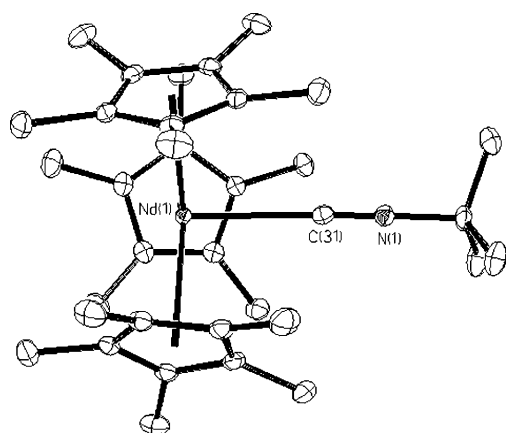


Figure 4. Thermal ellipsoid plot of complex **9** drawn at the 50% probability level. Hydrogen atoms and benzene solvent molecules have been omitted for clarity.

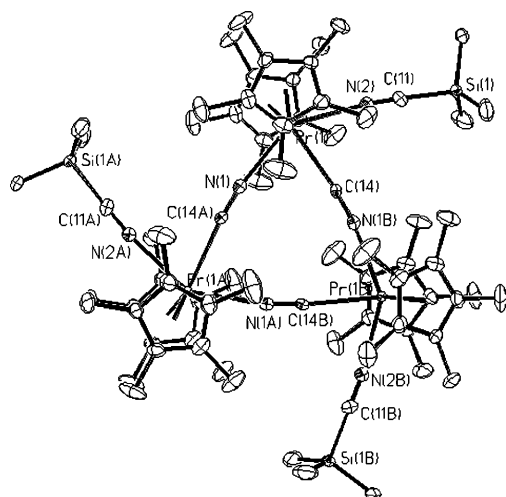
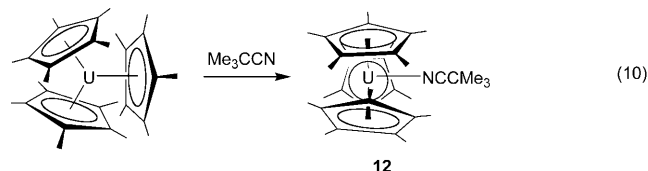


Figure 5. Thermal ellipsoid plot of complex **11** drawn at the 50% probability level. Hydrogen atoms and benzene solvent molecules have been omitted for clarity.

unit. Alternatively, Equation (7) could also be rationalized as a σ -bond metathesis (SBM) between a $\text{La}-(\eta^1\text{-C}_5\text{Me}_5)$ linkage and the $\text{Me}_3\text{Si-CN}$ bond. $[(\text{C}_5\text{Me}_5)_3\text{M}]$ complexes are known to react as σ -bonded $[(\text{C}_5\text{Me}_5)_2\text{M}(\eta^1\text{-C}_5\text{Me}_5)]$ complexes,^[1,2,4,16,21,22] and lanthanides have been shown to engage in SBM with silyl reagents,^[23–25] so the SBM reaction pathway is as viable as SIR.

$[(\text{C}_5\text{Me}_5)_3\text{U}(\text{NCCMe}_3)]$ (12**):** Previous isolation of $[(\text{C}_5\text{Me}_5)_3\text{U}(\text{CO})]$ ^[11] and $[(\text{C}_5\text{Me}_5)_3\text{U}(\text{N}_2)]$ ^[12] suggested that $[(\text{C}_5\text{Me}_5)_3\text{U}]$ would react with excess Me_3CCN to at least form a mono-nitrile adduct, $[(\text{C}_5\text{Me}_5)_3\text{U}(\text{NCCMe}_3)]$, analogous to **4** and **5**. In fact, since

the Shannon radius for U^{3+} (1.025 Å, six-coordinate) is intermediate between the radii for six-coordinate La^{3+} (1.032 Å) and Ce^{3+} (1.01 Å),^[26] the U^{3+} ion should be large enough to form a bis-nitrile complex, $[(\text{C}_5\text{Me}_5)_2\text{U}(\text{NCCMe}_3)_2]$, analogous to **1–3**. However, as shown in Equation (10), only the mono-nitrile adduct, **12**, was isolable under the conditions that formed **1–3**.



Complex **12** was characterized by ^1H NMR, ^{13}C NMR, and IR spectroscopy as well as by elemental analysis and by X-ray crystallography (Figure 6). The nitrile stretch in **12** is observed at 2245 cm^{-1} , slightly lower in energy than those observed in complexes **4** and **5**, at 2255 and 2256 cm^{-1} , respectively.

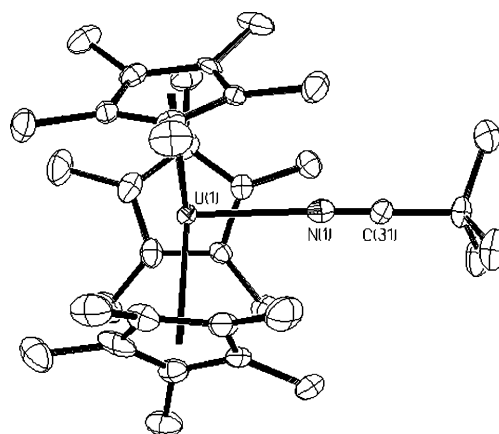
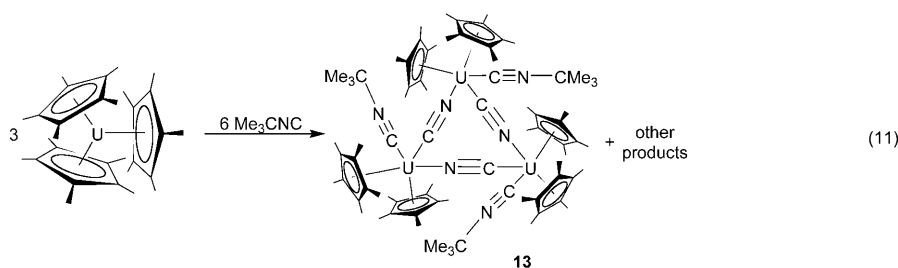


Figure 6. Thermal ellipsoid plot of complex **12** drawn at the 50% probability level. Hydrogen atoms and benzene solvent molecules have been omitted for clarity.

$[(\text{C}_5\text{Me}_5)_2\text{U}(\mu\text{-CN})(\text{CNCMe}_3)]_3$ (13**):** Unlike the lanthanum and neodymium complexes in Equations (5) and (6), $[(\text{C}_5\text{Me}_5)_3\text{U}]$ reacts with Me_3CNC to ultimately produce an N–C cleavage product, **13** [Eq. (11)], analogous to the lanthanum and praseodymium reactions with Me_3SiCN in Equation (7).



The initially isolated product of the $[(C_5Me_5)_3U]/CNCMe_3$ reaction is a soluble species with a single $(C_5Me_5)^-$ resonance in the 1H NMR spectrum and a single C–N stretch in the IR spectrum at 2137 cm^{-1} that may be the adduct $[(C_5Me_5)_3U(CNCMe_3)]$, but upon crystallization, the relatively insoluble cyanide trimer, **13**, is isolated. Complex **13** was characterized by IR spectroscopy, elemental analysis, and X-ray crystallography (Figure 7). Complex **13** displays

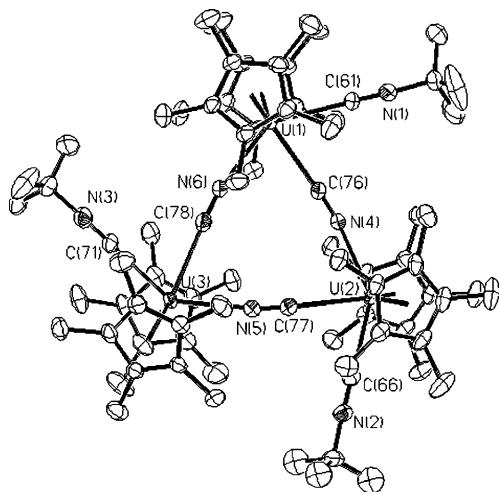


Figure 7. Thermal ellipsoid plot of complex **13** drawn at the 50% probability level. Hydrogen atoms and benzene solvent molecules have been omitted for clarity.

two C–N stretches in the IR spectrum at 2143 and 2088 cm^{-1} , which correspond to the coordinated isocyanide and the bridging cyanide ligands, respectively. The stretching mode of the bridging cyanide in **13** is similar to the 2082 cm^{-1} observed in the product of the reaction of $[(C_5Me_5)_2U(\mu-CN)]_n$ based on spectroscopic and analytical data.^[27] The 2143 cm^{-1} absorption of the coordinated isocyanide is not as high as the $2168\text{--}2179\text{ cm}^{-1}$ values found in the lanthanide isocyanide adducts, **8** and **9**, but it is still above the 2131 cm^{-1} value of the free isocyanide.

The C–N bond cleavage in Equation (11) could occur by means of sterically induced reduction or σ -bond metathesis through a $U-(\eta^1-C_5Me_5)$ intermediate. However, unlike Equation (7), neither $(C_5Me_5)_2$ nor $Me_3CC_5Me_5$ has been identified.

Structural analysis of complexes 2 and 3: Complexes **2** and **3** are isomorphous with the previously characterized $[(C_5Me_5)_3La(NCCMe_3)_2]$ (**1**). Complex **1** was the first example of a $[(C_5Me_5)_3ML_n]$ complex in which the three $(C_5Me_5)^-$ rings were not rigorously trigonal planar. Complexes **2** and **3** show that this occurs with other metals as well. All fourteen previously characterized metal complexes containing three $(\eta^5-C_5Me_5)^-$ ligands had a perfect trigonal-planar arrangement of the three ring centroids.

Hence, as in **1**, the three $(C_5Me_5 \text{ ring centroid})-M-(C_5Me_5 \text{ ring centroid})$ angles in **2** and **3**, 119.2 , 120.7 , 120.2° and 118.9 , 120.8 , 120.3° , respectively (Table 3), are not rigorously

Table 3. Selected bond lengths [\AA] and angles [$^\circ$] for complexes **1**, **2**, **3**, and **8** along with their six-coordinate M^{3+} ionic Shannon radii.^[26]

	1	2	3	8
M^{3+} ionic radius	1.032	1.01	0.99	1.032
M–C(C_5Me_5)	2.869(1)–	2.839(3)–	2.829(2)–	2.868(2)–
range	3.138(1)	3.136(3)	3.127(2)	3.141(2)
M–C(C_5Me_5) av	2.99(9)	2.97(10)	2.96(10)	2.99(9)
M–Cnt(1)	2.715	2.698	2.679	2.717
M–Cnt(2)	2.734	2.718	2.704	2.734
M–Cnt(3)	2.752	2.729	2.720	2.750
M–N(1)	2.681(1)	2.664(3)	2.636(1)	–
M–N(2)	2.656(1)	2.624(2)	2.613(1)	–
M–C(31)	–	–	–	2.779(2)
M–C(36)	–	–	–	2.747(2)
C(31)–N(1)	1.145(2)	1.138(4)	1.145(2)	1.153(2)
C(36)–N(2)	1.143(2)	1.134(4)	1.143(1)	1.152(2)
Cnt(1)–M–Cnt(2)	118.9	119.2	118.9	119.1
Cnt(1)–M–Cnt(3)	120.7	120.7	120.8	120.7
Cnt(2)–M–Cnt(3)	120.4	120.2	120.3	120.2
N(1)–M–N(2)	178.77(3)	178.61(7)	178.79(5)	–
C(31)–M–C(36)	–	–	–	178.67(5)
Cnt(1)–M–N(1)	91.0	90.9	90.8	–
Cnt(2)–M–N(1)	90.4	90.4	90.5	–
Cnt(3)–M–N(1)	88.3	88.2	88.4	–
Cnt(1)–M–N(2)	90.1	90.1	90.2	–
Cnt(2)–M–N(2)	89.5	90.0	89.6	–
Cnt(3)–M–N(2)	90.7	90.4	90.5	–
M out of Cnt ring plane	0.005	0.008	0.004	0.001

120° although they are close to 120° and reach a sum of 360° to give a trigonal-planar geometry of ring centroids. The metal centers in **2** and **3** are 0.008 and 0.004 \AA out of the plane of the three ring centroids compared with 0.005 \AA in **1**. The N(1)–M–N(2) angles of $178.61(7)$ and $178.79(5)^\circ$, for **2** and **3**, respectively, show the near linearity of the coordinated Me_3CCN ligands in the axial positions of the trigonal-bipyramidal geometry defined by the three ring centroids and the two nitrile donor atoms.

The M–(C_5Me_5 ring centroid) distances in **2** and **3**, 2.729 , 2.718 , 2.698 and 2.720 , 2.704 , 2.679 \AA , respectively, are approximately 0.1 \AA longer than those previously observed for the sterically crowded parent complexes, $[(C_5Me_5)_3Ce]$ and $[(C_5Me_5)_3Pr]$, 2.619 and 2.597 \AA , respectively (Table 4). Since the $[(C_5Me_5)_3Ln]$ parent complexes had metal–ring distances approximately 0.1 \AA longer than any previously observed pentamethylcyclopentadienyl lanthanides for those ions, the distances in **2** and **3** are quite extreme.

In contrast to these large Ln–(C_5Me_5 ring centroid) distances, the $2.664(3)$ and $2.636(1)\text{ \AA}$ Ln–N(1) and $2.624(2)$ and $2.613(1)\text{ \AA}$ Ln–N(2) bond lengths in **2** and **3**, respectively, are not unusually long. Analogous trends were observed with complex **1**,^[13] such that **1–3** are the first $[(C_5Me_5)_3ML_n]$ complexes that have a mixture of long and normal bond lengths. In all the previously identified $[(C_5Me_5)_3UL]$ and $[(C_5Me_5)_3UX]$ complexes, U–L and U–X were also unusual-

Table 4. Metal–(C₅Me₅) centroid [Å] and maximum methyl displacement out of the cyclopentadienyl plane [Å] for [(C₅Me₅)₃M], [(C₅Me₅)₃ML], and [(C₅Me₅)₃ML₂] complexes.

	Metal–(C ₅ Me ₅) centroid			Maximum methyl displacement
	max	median	min	
[(C ₅ Me ₅) ₃ La]	2.643	2.643	2.643	0.50
complex 1	2.752	2.734	2.715	0.43
complex 8	2.750	2.734	2.717	0.43
[(C ₅ Me ₅) ₃ Ce]	2.619	2.619	2.619	0.50
complex 2	2.729	2.718	2.698	0.43
[(C ₅ Me ₅) ₃ Pr]	2.597	2.597	2.597	0.52
complex 3	2.720	2.704	2.679	0.44
complex 4	2.658	2.640	2.620	0.52
[(C ₅ Me ₅) ₃ Nd]	2.582	2.582	2.582	0.52
complex 5	2.640	2.622	2.597	0.53
complex 9	2.638	2.620	2.599	0.54
[(C ₅ Me ₅) ₃ U] ^[8]	2.582	2.582	2.582	0.52
complex 12	2.645	2.623	2.603	0.54

ly long.^[9–12] The maximum displacement of the methyl groups from the (C₅Me₅)[−] ring plane, one of the characteristics used to evaluate sterically crowded complexes,^[28] are 0.43 and 0.44 Å for **2** and **3**, respectively. These are equivalent to that in **1**, 0.43 Å (Table 4).

Structural analysis of complexes 4, 5, and 12: Isomorphous complexes **4**, **5**, and **12** are similar to **1–3** in that the three (C₅Me₅)[−] rings do not rigorously define a trigonal plane, but the three (C₅Me₅ ring centroid)–M–(C₅Me₅ ring centroid) angles are again close to 120° (Table 5). However, in contrast to **1–3**, the sum of these three angles is slightly less than 360°, that is, 358.9, 358.6, and 359.1°, respectively, for **4**, **5**, and **12**. This is consistent with the fact that the metal atoms are further out of the plane defined by the three ring centroids: 0.161, 0.177, and 0.146 Å, respectively, for **4**, **5**, and **12**, relative to 0.004–0.008 Å for **1–3**. The distortion of the C₅Me₅ rings from trigonal-planar geometry is also

reflected in the 93.1–93.9° (C₅Me₅ ring centroid)–M–N(1) bond angles in **4**, **5**, and **12** compared to 88.2–91.0° for **1–3**.

The M–(C₅Me₅ ring centroid) distances in the mono-nitrile complexes **4**, **5**, and **12** are approximately 0.06 Å longer than those observed in their [(C₅Me₅)₃M] parent complexes (Table 4), that is, they are not as long as those observed in the bis-nitrile counterparts, **1–3**, but they are still much longer than conventional M–C(C₅Me₅) distances. The 2.557(3), 2.534(2), and 2.522(6) Å M–N bond lengths in complexes **4**, **5**, and **12**, respectively, are not unusually long and are slightly shorter than those observed in the bis-nitrile complexes **1–3**. The normal U–N(1) bond length in **12** is in sharp contrast to all the other [(C₅Me₅)₃UL] and [(C₅Me₅)₃UX] complexes observed to date.^[9–12]

Although the M–(C₅Me₅ ring centroid) distances of the [(C₅Me₅)₃M(NCCMe₃)] complexes are not as long as those in the [(C₅Me₅)₃M(NCCMe₃)₂] analogues, the maximum displacements of the methyl groups from the (C₅Me₅)[−] ring plane in **4**, **5**, and **12** (0.52, 0.53, and 0.54 Å, respectively) are larger than those in the bis-nitrile adducts. Comparison of the praseodymium complexes **3** and **4** in this regard is informative (Table 4). Although **3** has more ligands in its coordination sphere, the methyl displacements are smaller. Presumably this is because the rings are further away from each other in **3**.

Structural analysis of complex 8: The bis-isocyanide complex **8** is isomorphous with cyanide complexes **1–3**, with nearly identical Ln/C₅Me₅ bond lengths and angles to those observed in complex **1** (Table 3). The 2.779(2) and 2.747(2) Å La–C(31) and La–C(36) bond lengths in **8** are approximately 0.1 Å longer than the 2.681(1) and 2.656(1) Å La–N(1) and La–N(2) bond lengths observed in **1**. Lanthanide–isocyanide bonds are typically longer than lanthanide–nitrile bonds, as shown by the Ln–C and Ln–N bond lengths in [(C₅Me₅)₂Sm(μ-CN)(CNCMe₃)₃], 2.650 Å,^[29] and

Table 5. Selected bond lengths [Å] and angles [°] for complexes **4**, **5**, **9**, **12**, and [(C₅Me₅)₃U(N₂)] along with their six-coordinate M³⁺ ionic Shannon radii.^[26]

	4	5	9	12	[(C ₅ Me ₅) ₃ U(N ₂)]
M ³⁺ ionic radius	0.99	0.98	0.98	1.03	1.03
M–C(C ₅ Me ₅) range	2.823(4)–3.034(4)	2.814(2)–3.022(2)	2.815(1)–3.011(2)	2.811(7)–3.014(7)	2.823(2)–2.927(4)
M–C(C ₅ Me ₅) av	2.90(6)	2.88(6)	2.88(6)	2.89(6)	2.86(4)
M–Cnt(1)	2.640	2.622	2.620	2.623	2.588
M–Cnt(2)	2.620	2.597	2.599	2.603	2.588
M–Cnt(3)	2.658	2.640	2.638	2.645	2.588
M–N(1)	2.557(3)	2.534(2)	–	2.522(6)	2.49(1)
M–C(31)	–	–	2.602(2)	–	–
C(31)–N(1)	1.138(5)	1.140(2)	1.152(2)	1.142(8)	–
Cnt(1)–M–Cnt(2)	118.7	118.7	118.8	119.0	120
Cnt(1)–M–Cnt(3)	119.1	119.0	119.3	119.3	120
Cnt(2)–M–Cnt(3)	121.1	120.9	120.9	120.8	120
Cnt(1)–M–N(1)	93.4	93.8	93.2	93.1	90
Cnt(2)–M–N(1)	93.7	93.9	93.2	93.2	90
Cnt(3)–M–N(1)	93.4	93.9	93.6	93.3	90
N(1)–C(31)–C(32)	179.6(5)	179.4(2)	–	178.3(8)	–
C(31)–N(1)–C(32)	–	–	178.6(2)	–	–
M out of Cnt ring plane	0.161	0.177	0.153	0.146	0.000

$[(C_5Me_5)_2Sm(CNCMe_3)_2(\mu-O)]$, 2.62(1)/2.66(1) Å,^[30] compared with $[(C_5Me_5)_2Sm(\mu-CN)(NCCMe_3)_3]$, 2.557 Å,^[31] and $[(C_5Me_5)_2Sm(NCCMe_3)_2(\mu-O)]$, 2.530(3) and 2.545(3) Å.^[31] When compared with the M–C(CNR) bond lengths of 2.71, 2.70, and 2.65 Å in the substituted tris(cyclopentadienide) complexes, $[(MeC_5H_4)_3Ce(CNCMe_3)]$,^[32] $[(Me_3Si)_2C_5H_3]_3Ce(CNCMe_3)$,^[32] and $[(C_5H_5)_3Pr(CNC_6H_{11})]$,^[33] respectively, the La–C(31) and La–C(36) bond lengths in **8** are not unusually long when the differences in ionic radii between La^{3+} (1.32 Å), Ce^{3+} (1.25 Å), and Pr^{3+} (1.21 Å)^[26] are taken into account.

Structural analysis of complex 9: The mono-isocyanide complex **9** is isomorphous with the mono-nitrile complexes **4**, **5**, and **12**. As in the comparison of **8** with **1–3**, complex **9** has Ln/ C_5Me_5 bond lengths and angles nearly identical to those observed in complex **5** (Table 5). The 2.602(2) Å Nd–C(31) bond length in **9** is longer than the 2.534(2) Å Nd–N(1) bond length observed in **5**, which is consistent with the difference observed between **8** and **1**.

Structural analysis of complexes 10, 11, and 13: Isomorphous complexes **10**^[19] and **11** have normal bond parameters for lanthanide metallocenes (Table 6). As is typical in cy-

Table 7. Selected bond lengths [Å] and angles [°] for complex **13**.

	13
M–Cnt range	2.491–2.515
M–Cnt av	2.507
M–C(C_5Me_5) range	2.741(4)–2.834(4)
M–C(C_5Me_5) av	2.78(3)
M–C(CNCMe ₃) range	2.600(4)–2.632(4)
M–C(CNCMe ₃) av	2.62(2)
M–N,C(CN) range	2.582(3)–2.669(4)
M–N,C(CN) av	2.61(3)
N(CN)–C(CN) range	1.161(5)–1.168(5)
N(CN)–C(CN) av	1.164(3)
Cnt–M–Cnt range	134.7–136.6
Cnt–M–Cnt av	135.3
Cnt–M–N,C(CN) range	98.5–118.2
Cnt–M–N,C(CN) av	105.9
Cnt–M–C(CNCMe ₃) range	93.5–94.8
Cnt–M–C(CNCMe ₃) av	94.3
M–N,C(CN)–N,C(CN) range	176.1(3)–177.1(3)
M–N,C(CN)–N,C(CN) av	176.5(5)
N,C(CN)–M–N,C(CN) range	72.6(1)–72.9(1)
N,C(CN)–M–N,C(CN) av	72.8(2)

bond lengths in **8** were about 0.1 Å longer than the La–N(NCCMe₃) nitrile bond lengths in **1**.

Discussion

This study has shown that complex **1** is not the only sterically crowded $[(C_5Me_5)_3Ln]$ lanthanide complex that will add neutral ligands. Two additional ligands can be added to $[(C_5Me_5)_3Ce]$ and $[(C_5Me_5)_3Pr]$, and mono-ligand adducts are accessible with $[(C_5Me_5)_3Pr]$ and $[(C_5Me_5)_3Nd]$. Additionally, these results show that the formation of these $[(C_5Me_5)_3ML_2]$ and $[(C_5Me_5)_3ML]$ complexes is highly dependent upon the size of the metal and the nature of the coordinating ligand, as well as the 4f versus 5f electron configuration of the metal. As described below, some of the synthetic and structural trends are straightforward, but others are not.

For example, the addition of Me_3CCN to the $[(C_5Me_5)_3Ln]$ complexes [Eqs. (1)–(4)] to form 1) bis-nitrile $[(C_5Me_5)_3Ln(NCCMe_3)_2]$ complexes with the largest metals, La, Ce, and Pr, and 2) mono-nitrile $[(C_5Me_5)_3Ln(NCCMe_3)]$ complexes with the smaller metals, Pr and Nd, is quite reasonable once it was realized that two additional ligands could be added to the already sterically crowded $[(C_5Me_5)_3La]$.^[13] The fact that there is a metal of intermediate size that is the crossover point at which both mono- and bis-nitrile complexes are accessible (in this case, Pr) is also reasonable based on previously observed trends in lanthanide reactivity as a function of metal size.^[34] The observation of insertion chemistry with Sm and Y is consistent with the smaller size of these metals: presumably they are too sterically crowded to form $[(C_5Me_5)_3Ln(NCCMe_3)]$ complexes and their $(C_5Me_5)^-$ rings are more reactive due to the enhanced crowding.

Table 6. Selected bond lengths [Å] and angles [°] for complexes **10** and **11**.

	10	11
M–Cnt	2.562	2.515
M–C(C_5Me_5) range	2.799(2)–2.862(2)	2.754(7)–2.826(7)
M–C(C_5Me_5) av	2.83(2)	2.79(3)
M–N,C(CN)	2.671(3)–2.684(3)	2.619(8)–2.646(7)
M–N(NCSiMe ₃)	2.694(3)	2.644(7)
N(CN)–C(CN)	1.164(4)	1.188(11)
Cnt–M–Cnt	135.5	134.8
Cnt–M–N,C(CN)	98.7, 112.0	99.2, 112.3
Cnt–M–N(NCSiMe ₃)	94.1	94.0
M–N,C(CN)–N,C(CN)	171.0(3)	174.2(6)
N,C(CN)–M–N,C(CN)	75.00(9)	74.3(2)

nide-bridged complexes of these heavy metals, the C and N atoms of the cyanide cannot be differentiated and are modeled with 50% occupancy. Complex **13** is structurally similar to **10** and **11** (Table 7) but is not isomorphous. The U–(C_5Me_5 ring) parameters for **13** are very close to those of **11** even though the six-coordinate Shannon radius for U^{3+} is 1.03 Å compared with 0.99 Å for Pr^{3+} . For example, the M–C(C_5Me_5) averages are 2.78(3) Å for **13** and 2.79(3) Å for **11**, and the range of these bond lengths for **13**, 2.741(4)–2.834(4) Å, spans that for **11**, 2.754(7)–2.826(7) Å. The M–N,C(CN) bond lengths are also very similar, 2.582(3)–2.669(4) Å and 2.619(8)–2.646(7) Å for **13** and **11**, respectively. The uranium–isocyanide carbon bond lengths, 2.600(4)–2.632(4) Å, are smaller than the praseodymium–nitrile nitrogen bond length, 2.644(7) Å, even though U^{3+} has a larger ionic radius and the La–C(CNCMe₃) isocyanide

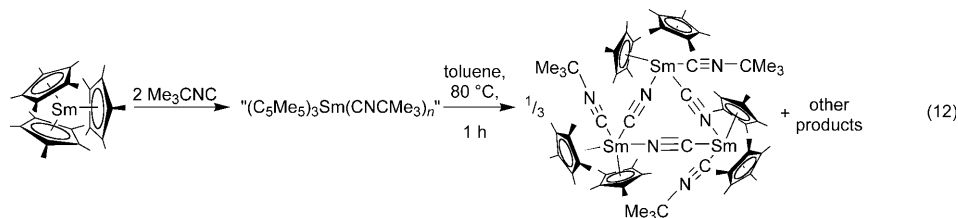
The structural details of complexes **1–5** are also self-consistent. The unusual features observed for complex **1** are also found for **2–5**. One of these is that the three ring centroids do not adopt a rigorously trigonal-planar arrangement that should give the most space to the rings. In contrast, all fourteen previously characterized $[(C_5Me_5)_3M]$,^[3–8] $[(C_5Me_5)_3ML]$,^[11,12] and $[(C_5Me_5)_3MX]$ ^[9,10,35] compounds adopted the trigonal-planar geometry for the three $(C_5Me_5)^-$ rings. Another unusual feature was the normal La–N bond lengths. All previously studied $[(C_5Me_5)_3ML]$ and $[(C_5Me_5)_3MX]$ complexes had M–L and M–X bond lengths almost 0.1 Å longer than normal. However, all of these previous examples were for M=U, and this study shows substantive differences in the chemistry of the $[(C_5Me_5)_3Ln]$ lanthanide complexes and $[(C_5Me_5)_3U]$.

Complexes **1–5** are unusual in that they are the first sterically crowded $[(C_5Me_5)_3M]$ complexes that contain a mixture of long and normal bond lengths. Since the Ln–(ring centroid) bond lengths are even longer than those in the $[(C_5Me_5)_3Ln]$ parent complexes, compounds **1–5** clearly have more steric congestion. However, the normal bond lengths of the nitriles suggest that ligands of the appropriate size can get close enough to the metal even in these crowded environments. With these strong σ -donor ligands adopting normal bond lengths, it is possible that the influence of the distant $(C_5Me_5)^-$ ligands is less important in determining the structure than in the $[(C_5Me_5)_3Ln]$ complexes in which they are the only ligands. In effect, the strong σ donors may attach to the metal and begin to push the $(C_5Me_5)^-$ to be outer sphere ligands, just as strong ligands like L=hexamethylphosphoramide can displace iodide ligands in LnI_3 to make outer sphere $[LnIL_n]^{2+}[(I)_2]^{2-}$ complexes.^[36,37] Hence, these complexes may represent a turning point in which the nitrile ligands, not the cyclopentadienyl ligands, are the primary influence on structure. The three ring centroids may distort from the most compact trigonal-planar geometry to accommodate steric bulk and packing of the *tert*-butyl substituents of the nitrile ligands rather than optimizing the geometry of the $[(C_5Me_5)_3]^{3-}$ ligand set.

The reactions of $[(C_5Me_5)_3La]$ and $[(C_5Me_5)_3Nd]$ with Me_3CNC to form complexes **8** and **9**, respectively, showed that analogous reactivity occurred with both nitrile and isocyanide reagents. This is consistent with the highly ionic character of the lanthanides. Both good σ donors and good π -acceptor ligands bind in the same way, primarily as σ donors. The C–N stretches of the isocyanide complexes are consistent with this picture.

The formation of a bis-isocyanide complex with lanthanum and a mono-isocyanide complex with the smaller neodymium matches the pattern observed with *tert*-butyl nitrile. However, as the lanthanide gets smaller, a change in nitrile

and isocyanide chemistry is observed. $[(C_5Me_5)_3Sm]$ reacts with Me_3CCN by insertion [Eq. (4)], but with Me_3CNC , initial coordination occurs and upon heating, the cyanide, $[(C_5Me_5)_2Sm(\mu-CN)(CNCMe_3)]_3$, was isolated in high yield [Eq. (12)].^[16] Hence, C–N cleavage occurs with the isocyanide rather than the insertion chemistry of the nitrile.



Cyanide formation also occurs with Me_3SiCN [Eq. (7)], a nitrile that has proven to be susceptible to cyanide formation in the past [Eq. (8)].^[19] It seems that the weaker Si–C bond of this nitrile is more susceptible to cleavage than Me_3CCN .

The reactions of $[(C_5Me_5)_3U]$ with nitriles and isocyanides are not directly analogous to those of the lanthanides and highlight the differences between the 4f and 5f elements.^[38] Although uranium is similar in size to lanthanum and cerium, and therefore presumably has the space to form bis-nitrile complexes like **1–3**, it only forms a mono-nitrile product, **12**, that is analogous to the praseodymium and neodymium complexes **4** and **5**. Since a bis-nitrile uranium product is sterically accessible, there may be an electronic reason why a second nitrile does not bind to **12**. This is currently under investigation.

Uranium also has the space to make isocyanide complexes like **8** and **9**. However, Equation (11) shows that N–C cleavage occurs to form the cyanide **13** as was observed with the smaller metal samarium in the lanthanide series [Eq. (12)].^[16] Formation of a uranium cyanide complex from Me_3CNC has previously been observed with the sterically normal $[(C_5Me_4H)_3U]$.^[39] That study found evidence for an adduct, $[(C_5Me_4H)_3U(CNCMe_3)]$, analogous to **9**, but it was unstable with respect to formation of the U^{4+} cyanide $[(C_5Me_4H)_3U(CN)]$, a compound that was crystallographically characterized as a 60:40 mixture with $[(C_5Me_4H)_3UCl]$.^[39] In that case, reductive cleavage of a C–N bond by U^{3+} presumably occurred. In Equation (11), no net U^{3+} reduction occurs since a trivalent product, **13**, is isolated. This is unusual since the U^{3+} ion in $[(C_5Me_5)_3U]$ should be more reducing than that in $[(C_5Me_4H)_3U]$. In the formation of **13** in Equation (11), apparently the ligand framework generates the chemistry. A predominance of steric over electronic factors was also used to explain CO stretching frequencies in $[(C_5Me_5)_3U(CO)]$ versus $[(C_5Me_4H)_3U(CO)]$.^[11]

The formation of uranium cyanide products in Equation (11) provides another interesting contrast with lanthanide complexes in Equations (5) and (6). In the

$[(C_5Me_5)_3U]/CNCMe_3$ reaction, it is the reductive reactivity of U^{3+} that causes the chemistry to differ from that of the Ln^{3+} ions. In contrast, with CO as a reagent, it is the stability of the U^{3+} CO complexes $[(C_5Me_5)_3U(CO)]^{[39]}$ and $[(C_5Me_5)_3U(CO)]^{[11]}$ that leads to formation of simple adducts rather than the insertion chemistry that occurs with $[(C_5Me_5)_3Ln]$ complexes to form the $[(C_5Me_5)_2Ln(O_2C_2Me_5)]$ nonclassical carbonium ion products.^[4,40] To date, the insertion reactivity found with $[(C_5Me_5)_3Ln]$ complexes has not been observed with $[(C_5Me_5)_3U]$. Only adduct formation or reduction has occurred.

Conclusion

The reactions between $[(C_5Me_5)_3M]$ complexes and Me_3CCN produce a series of sterically crowded complexes $[(C_5Me_5)_3M(NCCMe_3)_n]$ ($n=1, 2$) in which the number of coordinated nitrile ligands depends upon the size of the metal center and its 4f versus 5f electron configuration. When M is a lanthanide, the larger metals La and Ce have $n=2$, the intermediate metal Pr can have $n=1$ or 2, and the smaller metal Nd has $n=1$. When M is uranium, the $n=1$ product analogous to those with Pr and Nd is isolated, although the size of U is comparable to that of La and Ce. When M is Sm and Y, insertion chemistry to form $[(C_5Me_5)_2Ln\{NC(C_5Me_5)(CMe_3)\}(NCCMe_3)]$ occurs.

The reactions between $[(C_5Me_5)_3M]$ lanthanide complexes and the isocyanide Me_3CNC are similar to the nitrile chemistry in that La and Nd make $[(C_5Me_5)_3Ln(CNCMe_3)_n]$ complexes with $n=2$ and 1, respectively, and Sm differs. In the samarium isocyanide case, a cyanide trimer is formed, $[(C_5Me_5)_2Sm(\mu-CN)(CNCMe_3)_3]$. As in the case of the nitrile, the isocyanide uranium chemistry is not analogous to the lanthanide results. $[(C_5Me_5)_3U]$ does not form isocyanide adducts like La and Nd, but instead forms a cyanide trimer, $[(C_5Me_5)_2U(\mu-CN)(CNCMe_3)_3]$, which is analogous to the Sm product. These reactions indicate that subtle factors involving the particular $[(C_5Me_5)_3M]$ complex/substrate combination affect the course of these reactions.

The structural data for these new complexes show that complexes more sterically crowded than the $[(C_5Me_5)_3M]$ compounds can be synthesized, but they adopt structures in which both unusually long and normal metal–ligand bond lengths are observed. The reactivity consequences of these mixed bond lengths in sterically crowded complexes are under investigation.

Experimental Section

The syntheses and manipulations described below were conducted under argon or nitrogen with rigorous exclusion of air and water using glove box, vacuum line, and Schlenk techniques. Solvents were dried over columns containing Q-5 (Englehardt Chemical Inc.) and molecular sieves. NMR spectroscopic solvents were dried with a sodium–potassium alloy, degassed, and vacuum transferred prior to use. Me_3CCN , Me_3CNC , and

Me_3SiCN were distilled onto 4 Å molecular sieves and degassed by three freeze–pump–thaw cycles before use. The $[(C_5Me_5)_3M]$ complexes ($M=La^{[3]} Ce^{[4]} Pr^{[4]} Nd^{[5]} Sm^{[6]} Y^{[7]} U^{[8]}$) were prepared as previously described. 1H and ^{13}C NMR spectra were obtained using a Bruker DRX 500 MHz spectrometer at 25 °C. IR samples were prepared as KBr pellets and the spectra were obtained using a Varian 1000 FTIR system. Elemental analyses were performed using a Perkin–Elmer 2400 CHNS analyzer.

Complex 2: Me_3CCN (110 μL , 1.00 mmol) was added with a syringe to a stirred solution of $[(C_5Me_5)_3Ce]$ (254 mg, 0.47 mmol) in toluene (10 mL). An immediate color change from green to bright yellow was observed. After 30 min, the solvent was removed under reduced pressure to yield a bright yellow powder (329 mg, 99 %). Bright yellow crystals of X-ray quality were grown from a concentrated solution of the powder in benzene at 25 °C. 1H NMR (C_6D_6): $\delta=3.69$ (s, $\Delta\nu_{1/2}=9$ Hz, 45H; C_5Me_5), -0.87 ppm (s, $\Delta\nu_{1/2}=24$ Hz, 18H; Me_3CCN); ^{13}C NMR (C_6D_6): $\delta=154.23$ (C_5Me_5), 26.47 (Me_3CCN), 21.76 (Me_3CCN), 19.07 (Me_3CCN), 8.25 ppm (C_5Me_5); IR: $\tilde{\nu}=2976$ (s), 2904 (s), 2855 (s), 2718 (w), 2255 (m), 1476 (m), 1459 (m), 1439 (m), 1401 (w), 1371 (m), 1238 (m), 1016 (w), 947 (w), 802 (w), 730 (w), 695 cm^{-1} (w); elemental analysis calcd (%) for $C_{40}H_{63}N_2Ce$: C 67.47, H 8.92, N 3.93; found: C 67.23, H 8.69, N 3.31.

Complex 3: Me_3CCN (16 μL , 0.14 mmol) was added with a syringe to a stirred solution of $[(C_5Me_5)_3Pr]$ (37 mg, 0.068 mmol) in toluene (5 mL). An immediate color change from dark orange to pale yellow was observed. After 30 min, the solvent was removed under reduced pressure to yield a pale yellow powder (48 mg, 99 %). Pale yellow crystals of X-ray quality were grown from a concentrated solution of the powder in benzene at 25 °C. 1H NMR (C_6D_6): $\delta=8.17$ (s, $\Delta\nu_{1/2}=10$ Hz, 45H; C_5Me_5), -15.70 ppm (s, $\Delta\nu_{1/2}=237$ Hz, 18H; Me_3CCN); ^{13}C NMR (C_6D_6): $\delta=0.24$ ppm (C_5Me_5); IR: $\tilde{\nu}=2976$ (s), 2903 (s), 2855 (s), 2719 (w), 2255 (m), 1476 (m), 1458 (m), 1439 (m), 1371 (m), 1238 (m), 1017 (w), 947 (w), 869 (w), 804 (w), 729 (w), 695 cm^{-1} (w); elemental analysis calcd (%) for $C_{40}H_{63}N_2Pr$: C 67.40, H 8.91, N 3.93; found: C 67.46, H 8.35, N 3.22.

Complex 4: Me_3CCN (21 μL , 0.19 mmol) was added with a syringe to a stirred solution of $[(C_5Me_5)_3Pr]$ (103 mg, 0.19 mmol) in toluene (10 mL). An immediate color change from dark orange to pale yellow was observed that was indistinguishable from that of **3**. After 30 min, the solvent was removed under reduced pressure to yield a pale yellow powder (118 mg, 99 %). Pale yellow crystals of X-ray quality were grown from a concentrated solution of the powder in benzene at 25 °C. 1H NMR (C_6D_6): $\delta=8.19$ (s, $\Delta\nu_{1/2}=8$ Hz, 45H; C_5Me_5), -15.35 ppm (s, $\Delta\nu_{1/2}=59$ Hz, 9H; Me_3CCN); ^{13}C NMR (C_6D_6): $\delta=0.24$ ppm (C_5Me_5); IR: $\tilde{\nu}=2976$ (s), 2903 (s), 2855 (s), 2719 (w), 2255 (m), 1476 (m), 1458 (m), 1439 (m), 1371 (m), 1238 (m), 1017 (w), 947 (w), 869 (w), 804 (w), 729 (w), 695 cm^{-1} (w); elemental analysis calcd (%) for $C_{35}H_{54}NPr$: C 66.76, H 8.64, N 2.22; found: C 66.19, H 9.44, N 2.03.

Complex 5: Me_3CCN (130 μL , 1.18 mmol) was added with a syringe to a stirred solution of $[(C_5Me_5)_3Nd]$ (315 mg, 0.57 mmol) in toluene (5 mL). An immediate color change from yellow brown to mint green was observed. After 30 min, the solvent was removed under reduced pressure to yield a mint green powder (361 mg, 99 %). Mint green crystals of X-ray quality were grown from a concentrated solution of the powder in benzene at 25 °C. 1H NMR (C_6D_6): $\delta=9.23$ (s, $\Delta\nu_{1/2}=9$ Hz, 45H; C_5Me_5), -8.68 ppm (s, $\Delta\nu_{1/2}=29$ Hz, 9H; Me_3CCN); ^{13}C NMR (C_6D_6): $\delta=229.76$ (C_5Me_5), 214.15 (C_5Me_5), 6.14 ppm (Me_3CCN); IR: $\tilde{\nu}=2976$ (s), 2903 (s), 2855 (s), 2718 (m), 2256 (m), 1475 (m), 1458 (m), 1439 (m), 1371 (m), 1238 (m), 1206 (w), 1161 (w), 1016 (m), 947 (w), 869 (w), 805 (w), 733 (m), 696 cm^{-1} (m); elemental analysis calcd (%) for $C_{35}H_{54}NNd$: C 66.40, H 8.60, N 2.21; found: C 65.87, H 8.59, N 2.17.

Complex 6: Me_3CCN (75 μL , 0.68 mmol) was added with a syringe to a stirred solution of $[(C_5Me_5)_3Sm]$ (126 mg, 0.23 mmol) in toluene (5 mL). An immediate color change from brown to orange was observed. After 30 min, the solvent was removed under reduced pressure to yield an orange powder (163 mg, 99 %). 1H NMR (C_6D_6): $\delta=3.07$ (s, 6H; C_5Me_5), 2.21 (s, 3H; C_5Me_5), 1.86 (s, 6H; C_5Me_5), 1.62 (s, $\Delta\nu_{1/2}=10$ Hz, 30H; C_5Me_5), 0.23 (s, 9H; Me_3CCN), -0.61 ppm (s, 9H; Me_3CCN); ^{13}C NMR (C_6D_6): $\delta=111.78$ (C_5Me_5), 33.52 (C_5Me_5), 26.67 (Me_3CCN), 15.84 (C_5Me_5), 14.69 (C_5Me_5), 12.32 ppm (C_5Me_5); IR: $\tilde{\nu}=2960$ (s), 2907 (s),

2855 (s), 2721 (w), 2262 (m), 1624 (s), 1591 (m), 1477 (m), 1460 (m), 1443 (m), 1374 (m), 1352 (m), 1240 (m), 1207 (w), 1123 (w), 1059 (w), 1021 (m), 925 (m), 801 (w), 730 (w), 695 cm⁻¹ (w); elemental analysis calcd (%) for C₄₀H₆₃N₂Sm: C 66.51, H 8.79, N 3.88; found: C 65.57, H 9.46, N 3.52.

Complex 7: Me₃CCN (45 µL, 0.41 mmol) was added with a syringe to a stirred solution of [(C₅Me₅)₃Y] (90 mg, 0.18 mmol) in methycyclohexane (5 mL). An immediate color change from orange to yellow was observed. After 30 min, the solvent was removed under reduced pressure to yield a yellow powder (120 mg, 99%). ¹H NMR (C₆D₆): δ = 2.14, (s, 3H; C₅Me₅), 2.11 (s, 30H; C₅Me₅), 1.89 (s, 6H; C₅Me₅), 1.30 (s, 6H; C₅Me₅), 0.78 ppm (s, 18H; Me₃CCN); ¹³C NMR (C₆D₆): δ = 142.26 (C₅Me₅), 134.42 (C₅Me₅), 118.22 (Me₃CCN), 115.25 (C₅Me₅), 114.70 (Me₃CCN), 31.48 (C₅Me₅), 28.49 (C₅Me₅), 27.53 (CCMe₃), 13.64 (C₅Me₅), 12.57 (C₅Me₅), 12.31 (Me₃CCN), 11.93 (C₅Me₅), 11.80 ppm (Me₃CCN); IR: ν̄ = 2957 (s), 2909 (s), 2856 (s), 2723 (w), 2264 (m), 1628 (s), 1591 (m), 1477 (m), 1458 (m), 1445 (m), 1373 (m), 1352 (m), 1240 (m), 1207 (w), 1143 (w), 1059 (w), 1023 (m), 928 (m), 851 (w), 802 (w), 697 (w), 652 cm⁻¹ (m); elemental analysis calcd (%) for C₄₀H₆₃N₂Y: C 72.70, H 9.61, N 4.24; found: C 71.89, H 9.57, N 3.66.

Complex 8: Me₃CNC (55 µL, 0.49 mmol) was added with a syringe to a stirred solution of [(C₅Me₅)₃La] (110 mg, 0.20 mmol) in toluene (5 mL). An immediate color change from yellow to colorless was observed. After 30 min, the solvent was removed under reduced pressure to yield a colorless powder (142 mg, 99%). Colorless crystals of X-ray quality were grown from a concentrated solution of the powder in benzene at 25 °C. ¹H NMR (C₆D₆): δ = 2.17 (s, 45H; C₅Me₅), 1.02 ppm (s, 18H; Me₃CNC); ¹³C NMR (C₆D₆): δ = 137.88 (Me₃CNC), 118.86 (C₅Me₅), 55.65 (Me₃CNC), 30.05 (Me₃CNC), 13.46 ppm (C₅Me₅); IR: ν̄ = 2982 (s), 2902 (s), 2854 (s), 2718 (w), 2168 (s), 2128 (w), 1495 (m), 1475 (m), 1448 (s), 1438 (s), 1400 (m), 1372 (s), 1237 (m), 1202 (s), 1018 (w), 852 (w), 731 (m), 697 cm⁻¹ (m); elemental analysis calcd (%) for C₄₀H₆₃N₂La: C 67.59, H 8.93, N 3.94; found: C 67.15, H 8.45, N 3.20.

Complex 9: Me₃CNC (17 µL, 0.15 mmol) was added with a syringe to a stirred solution of [(C₅Me₅)₃Nd] (41 mg, 0.075 mmol) in toluene (4 mL). An immediate color change from yellow-brown to mint green was observed. After 30 min, the solvent was removed under reduced pressure to yield a mint green powder (47 mg, 99%). Mint green crystals of X-ray quality were grown from a concentrated solution of the powder in benzene at 25 °C. ¹H NMR (C₆D₆): δ = 9.07 (s, Δν_{1/2} = 9 Hz, 45H; C₅Me₅), -8.08 ppm (s, Δν_{1/2} = 70 Hz, 9H; Me₃CNC); ¹³C NMR (C₆D₆): δ = 228.58 (C₅Me₅), 212.78 (C₅Me₅), 9.60 ppm (Me₃CCN); IR: ν̄ = 2979 (s), 2903 (s), 2855 (s), 2719 (w), 2178 (s), 1471 (m), 1438 (m), 1400 (w), 1372 (m), 1237 (w), 1201 (m), 1084 (w), 1057 (w), 1017 (w), 948 (w), 850 (w), 802 (w), 730 (w), 702 cm⁻¹ (w); elemental analysis calcd (%) for C₃₅H₅₄NdN₂: C 66.40, H 8.60, N 2.21; found: C 66.68, H 8.75, N 2.13.

Complex 10: Me₃SiCN (6.5 µL, 0.052 mmol) was added with a syringe to a solution of [(C₅Me₅)₃La] (14 mg, 0.026 mmol) in C₆D₆ (1 mL). An immediate color change from yellow to colorless was observed. The ¹H NMR spectrum showed two products, which were identified as the previously characterized [(C₅Me₅)₂La(μ-CN)(NCSiMe₃)₃]^[19] and Me₃Si(C₅Me₅)^[18]. Complex **10** was also identified from this reaction by X-ray crystallography.

Complex 11: Me₃SiCN (26 µL, 0.21 mmol) was added with a syringe to a stirred solution of [(C₅Me₅)₃Pr] (56 mg, 0.10 mmol) in toluene (5 mL). An immediate color change from orange to yellow was observed. After stirring for 30 min, the solvent was removed under reduced pressure to yield a tacky yellow solid, which was washed with hexane to yield a yellow powder (76 mg, 99%). Yellow crystals of X-ray quality were grown from a concentrated solution of the powder in benzene at 25 °C. When the reaction was carried out in a sealed J. Young tube, the ¹H NMR spectrum showed two clean products in a 1:1 ratio, one of which matched that of the previously characterized Me₃Si(C₅Me₅)^[18]. ¹H NMR (C₆D₆): δ = 4.40 (s, Δν_{1/2} = 58 Hz, 9H; SiMe₃), -5.72 ppm (s, Δν_{1/2} = 177 Hz, 30H; C₅Me₅); ¹³C NMR data was not obtained due to the poor solubility of **11** in organic solvents (THF, benzene, and toluene); IR: ν̄ = 2971 (s), 2907 (s), 2859 (s), 2728 (w), 2179 (m), 2108 (m), 1493 (w), 1480 (w), 1438 (m), 1384 (m), 1259 (w), 1062 (w), 1021 (m), 844 (w),

802 (w), 729 (w), 676 cm⁻¹. Elemental analysis was consistent with the base-free adduct [(C₅Me₅)₂Pr(μ-CN)]₃; elemental analysis calcd (%) for C₆₃H₉₀N₃Pr₃: C 57.67, H 6.91, N 3.20; found: C 57.21, H 6.72, N 2.70.

Complex 12: Me₃CCN (100 µL, 0.90 mmol) was added with a syringe to a stirred solution of [(C₅Me₅)₃U] (290 mg, 0.45 mmol) in toluene (5 mL). A color change from brown to dark brown was observed. After 30 min, the solvent was removed under reduced pressure to yield a dark brown powder (325 mg, 99%). Dark brown crystals of X-ray quality were grown from a concentrated solution of the powder in benzene at 25 °C. ¹H NMR (C₆D₆): δ = 2.28 (s, Δν_{1/2} = 7 Hz, 45H; C₅Me₅), -12.31 ppm (s, Δν_{1/2} = 267 Hz, 9H; Me₃CCN); ¹³C NMR (C₆D₆): δ = 286.28 (C₅Me₅), -83.79 ppm (C₅Me₅); IR: ν̄ = 2964 (s), 2904 (s), 2856 (s), 2720 (w), 2245 (w), 1656 (w), 1606 (w), 1573 (w), 1475 (m), 1458 (m), 1438 (m), 1372 (m), 1237 (m), 1206 (w), 1019 (w), 944 (w), 729 (w), 703 cm⁻¹ (w); elemental analysis calcd (%) for C₃₅H₅₄NU: C 57.84, H 7.49, N 1.93; found: C 57.11, H 7.25, N 2.00.

Complex 13: Me₃CNC (25 µL, 0.22 mmol) was added with a syringe to a stirred solution of [(C₅Me₅)₃U] (52 mg, 0.081 mmol) in toluene (5 mL). A color change from brown to dark brown was observed. After 30 min, the solvent was removed under reduced pressure to yield a dark brown powder (58 mg), which exhibited a single ¹H NMR spectroscopic resonance (C₆D₆) at δ = 1.20 ppm. Dark brown crystals of X-ray quality were grown from a concentrated solution of the powder in benzene at 25 °C (38 mg, 76%). NMR spectroscopic data for **13** was not obtained due to the poor solubility in organic solvents (THF, benzene, and toluene). IR: ν̄ = 2983 (s), 2896 (s), 2854 (s), 2721 (w), 2143 (s), 2088 (m), 1437 (m), 1372 (m), 1235 (w), 1207 (m), 1021 (w), 855 (w), 730 (w), 710 (w), 696 cm⁻¹ (w); elemental analysis calcd (%) for C₇₈H₁₁₇N₆U₃: C 50.56, H 6.36, N 4.54; found: C 51.05, H 6.45, N 4.13.

CCDC-735585 (**2**), -735586 (**3**), -735587 (**4**), -735588 (**5**), -735589 (**8**), -735590 (**9**), -735591 (**11**), -735592 (**12**), and -735593 (**13**) contain the supplementary crystallographic data for this paper. These data can be obtained free of charge from The Cambridge Crystallographic Data Centre via www.ccdc.cam.ac.uk/data_request/cif.

Acknowledgements

We thank the National Science Foundation for support of this research and Michael K. Takase for his assistance with X-ray crystallography.

- [1] W. J. Evans, B. L. Davis, *Chem. Rev.* **2002**, *102*, 2119–2136.
- [2] W. J. Evans, *Inorg. Chem.* **2007**, *46*, 3435–3449.
- [3] W. J. Evans, B. L. Davis, J. W. Ziller, *Inorg. Chem.* **2001**, *40*, 6341–6348.
- [4] W. J. Evans, J. M. Perotti, S. A. Kozimor, T. M. Champagne, B. L. Davis, G. W. Nyce, C. H. Fujimoto, R. D. Clark, M. A. Johnston, J. W. Ziller, *Organometallics* **2005**, *24*, 3916–3931.
- [5] W. J. Evans, C. A. Seibel, J. W. Ziller, *J. Am. Chem. Soc.* **1998**, *120*, 6745–6752.
- [6] W. J. Evans, S. L. Gonzales, J. W. Ziller, *J. Am. Chem. Soc.* **1991**, *113*, 7423–7424.
- [7] W. J. Evans, B. L. Davis, T. M. Champagne, J. W. Ziller, *Proc. Natl. Acad. Sci. USA* **2006**, *103*, 12678–12683.
- [8] W. J. Evans, K. J. Forrestal, J. W. Ziller, *Angew. Chem.* **1997**, *109*, 798–799; *Angew. Chem. Int. Ed. Engl.* **1997**, *36*, 774–776.
- [9] W. J. Evans, G. W. Nyce, M. A. Johnston, J. W. Ziller, *J. Am. Chem. Soc.* **2000**, *122*, 12019–12020.
- [10] W. J. Evans, S. A. Kozimor, J. W. Ziller, *Organometallics* **2005**, *24*, 3407–3412.
- [11] W. J. Evans, S. A. Kozimor, G. W. Nyce, J. W. Ziller, *J. Am. Chem. Soc.* **2003**, *125*, 13831–13835.
- [12] W. J. Evans, S. A. Kozimor, J. W. Ziller, *J. Am. Chem. Soc.* **2003**, *125*, 14264–14265.
- [13] W. J. Evans, T. J. Mueller, J. W. Ziller, *J. Am. Chem. Soc.* **2009**, *131*, 2678–2686.

- [14] V. Chebolu, R. R. Whittle, A. Sen, *Inorg. Chem.* **1985**, *24*, 3082–3085.
- [15] K. J. Forrestal, Ph.D. Thesis, University of California, Irvine, **1997**.
- [16] W. J. Evans, K. J. Forrestal, J. W. Ziller, *J. Am. Chem. Soc.* **1998**, *120*, 9273–9282.
- [17] W. G. Van Der Sluys, A. P. Sattelberger, *Inorg. Chem.* **1989**, *28*, 2496–2498.
- [18] G. H. Llinás, M. Mena, F. Palacios, P. Royo, R. Serrano, *J. Organomet. Chem.* **1988**, *340*, 37–40.
- [19] W. J. Evans, E. Montalvo, T. M. Champagne, J. W. Ziller, A. G. DiPasquale, A. L. Rheingold, *Organometallics* **2009**, *28*, 2897–2903.
- [20] W. J. Evans, G. W. Nyce, R. D. Clark, R. J. Doedens, J. W. Ziller, *Angew. Chem.* **1999**, *111*, 1917–1919; *Angew. Chem. Int. Ed.* **1999**, *38*, 1801–1803.
- [21] W. J. Evans, K. J. Forrestal, J. W. Ziller, *J. Am. Chem. Soc.* **1995**, *117*, 12635–12636.
- [22] W. J. Evans, K. J. Forrestal, J. W. Ziller, *Angew. Chem.* **1997**, *109*, 798–799; *Angew. Chem. Int. Ed. Engl.* **1997**, *36*, 774–776.
- [23] I. Castillo, T. D. Tilley, *Organometallics* **2000**, *19*, 4733–4739.
- [24] N. S. Radu, T. D. Tilley, A. L. Rheingold, *J. Organomet. Chem.* **1996**, *516*, 41–49.
- [25] N. S. Radu, T. D. Tilley, A. L. Rheingold, *J. Am. Chem. Soc.* **1992**, *114*, 8293–8295.
- [26] R. D. Shannon, *Acta. Crystallogr. Sect. A* **1976**, *32*, 751–767.
- [27] J. Maynadié, J. Berthet, P. Thuery, M. Ephritikhine, *Organometallics* **2007**, *26*, 2623–2629.
- [28] W. J. Evans, S. A. Kozimor, J. W. Ziller, *Inorg. Chem.* **2005**, *44*, 7960–7969.
- [29] W. J. Evans, D. K. Drummond, *Organometallics* **1988**, *7*, 797–802.
- [30] W. J. Evans, D. K. Drummond, L. A. Hughes, H. Zhang, J. L. Atwood, *Polyhedron* **1988**, *7*, 1693–1703.
- [31] W. J. Evans, E. Montalvo, S. E. Foster, K. A. Harada, J. W. Ziller, *Organometallics* **2007**, *26*, 2904–2910.
- [32] S. D. Stults, R. A. Andersen, A. Zalkin, *Organometallics* **1990**, *9*, 115–122.
- [33] J. H. Burns, W. H. Baldwin, *J. Organomet. Chem.* **1976**, *120*, 361–368.
- [34] R. Anwender, W. A. Herrmann, *Top. Curr. Chem.* **1996**, *179*, 1–32.
- [35] W. J. Evans, G. W. Nyce, J. W. Ziller, *Organometallics* **2001**, *20*, 5489–5491.
- [36] Z. Hou, Y. Wakatsuki, *J. Chem. Soc. Chem. Commun.* **1994**, 1205–1206.
- [37] W. J. Evans, R. N. R. Broomhall-Dillard, J. W. Ziller, *Polyhedron* **1998**, *17*, 3361–3370.
- [38] a) T. Arliguie, L. Belkhir, S. Bouaoud, P. Thuery, C. Villiers, A. Boucekkine, M. Ephritikhine, *Inorg. Chem.* **2009**, *48*, 221–230; b) M. Roger, N. Barros, T. Arliguie, T. Pierre, L. Maron, M. Ephritikhine, *J. Am. Chem. Soc.* **2006**, *128*, 8790–8802; c) T. Mehdoui, J. Berthet, P. Thuery, L. Salmon, E. Riviere, M. Ephritikhine, *Chem. Eur. J.* **2005**, *11*, 6994–7006; d) T. Mehdoui, J. Berthet, P. Thuery, M. Ephritikhine, *Eur. J. Inorg. Chem.* **2004**, 1996–2000; e) C. Villiers, P. Thuery, M. Ephritikhine, *Eur. J. Inorg. Chem.* **2004**, 4624–4632; f) T. Mehdoui, J. Berthet, P. Thuery, M. Ephritikhine, *Dalton Trans.* **2004**, 579–590; g) J. G. Brennan, S. D. Stults, R. A. Andersen, A. Zalkin, *Inorg. Chim. Acta* **1987**, *139*, 201–202; h) J. G. Brennan, S. D. Stults, R. A. Andersen, A. Zalkin, *Organometallics* **1988**, *7*, 1329–1334.
- [39] M. del Mar Conejo, J. S. Parry, E. Carmona, M. Schultz, J. G. Brennan, S. M. Beshouri, R. A. Andersen, R. D. Rogers, S. Coles, M. Hursthouse, *Chem. Eur. J.* **1999**, *5*, 3000–3009.
- [40] W. J. Evans, K. J. Forrestal, J. W. Ziller, *J. Am. Chem. Soc.* **1995**, *117*, 12635–12636.

Received: July 18, 2009

Published online: November 27, 2009